ISSN (Online) : 2319 - 8753
ISSN (Print) : 2347 - 6710

International Journal of Innovative Research in Science, Engineering and Technology

Volume 3, Special Issue 3, March 2014

2014 International Conference on Innovations in Engineering and Technology (ICIET'14)

On 21st & 22nd March Organized by

K.L.N. College of Engineering, Madurai, Tamil Nadu, India

Power Optimization Strategy of a Cascaded Dc/Dc Converter Topologies for Grid Connected Photo Voltaic System

Ganga. M

Kings College of engineering, TamilNadu, India.

ABSTRACT—solar energy is present throughout the day but the solar irradiation levels vary due to sun intensity and unpredictable shadows cast by clouds, birds, trees, etc. The common inherent drawback of photovoltaic systems is their intermittent natures that make them unreliable. Moreover, most PV modules are designed for stand-alone applications that have output voltage adapted to lead batteries. Indeed, this historical sizing of PV modules can be discussed in the case of grid-connected systems. In this paper, a cascaded dc/dc converter based on boost chopper is proposed. The global optimum of cascaded connections of PV modules is generally equivalent with operating all the modules at maximum power point tracking (MPPT). This topology will be optimized to maximize the efficiency or minimize the volume. The originality of this optimization is that the converter's parameters and the arrangement of the PV cells are variable parameters. Indeed, the optimization is done on the entire system. The optimization uses a maximum power point tracking (MPPT) algorithm. Finally, optimized topologies connected to several PV are evaluated at different situations of typical shadows.

INDEX TERMS−DC/DC converter, optimization, photovoltaic, power electronics, and shades.

I. INTRODUCTION

In the context of a continuously changing economic, political and social environment, the ways of obtaining energy cheaply and safely is an issue of extreme importance. Nowadays world pays growing attention to the renewable energy sources, clean and practically inexhaustible, and makes efforts to sustain the improvement of the existing conversion technologies and the development of new ones [1], [2]. In particular, photovoltaic (PV) installations are an already familiar landscape, either as small (less than 5 kW) residential stand-alone or even grid-connected, or as larger (hundreds of kW), One of the most important aspects is the *maximum power point tracking* (MPPT), aiming at maximizing the extracted energy irrespective of the irradiance conditions [9]. A lot of work has been done in order to find simple, efficient and minimal knowledge-demanding methods of MPPT [10], [11], [12], from

which a successful one is the so-called *perturb-and observe* (P&O) method. The proposed solution will have to decrease the effects of shadow and keep the reliability and the cost imposed by the market [6]–[9]. This work focuses on the choice of different stages of conversion and the arrangement of the PV cells.

II. STUDIED PV FIELD TOPOLOGY

The state of the art has revealed numerous advantages of cascaded dc/dc converters between PV modules and the inverter to reduce the impact of shadow and maximize the produced energy [10]. The boost converter has become of great interest in this field topology. Indeed, its voltage rising, its high efficiency, its reliability, the possibility of implementing a MPPT, and its low price are decisive advantages [11], [12]. Thus, numerous interests can be brought by this field topology (see Fig. 1). This topology will be studied in this paper. Moreover, the historical stand-alone applications have led to a PV module's output adapted to the lead battery (12 or 24 V). This sizing can be discussed for grid-connected applications; however, few papers reconsider it. Nowadays, power electronics is optimized with industrial PV modules.

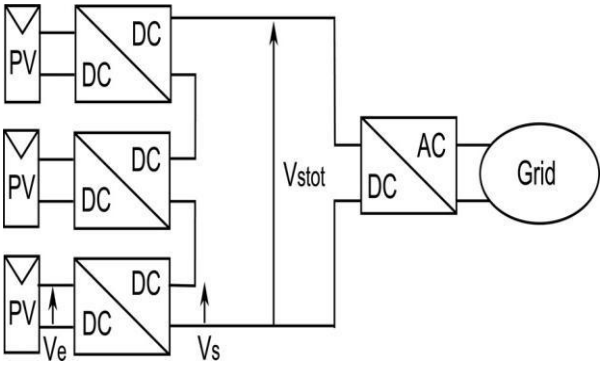

Fig. 1. Studied PV field topology.

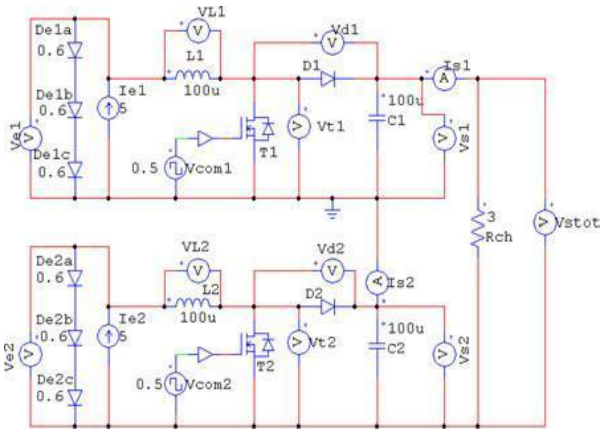

Fig. 2. PSIM simulations scheme.

This work develops two main originalities:

1) The optimization is made on the entire system;

2) The historical PV sizing is reconsidered.

The dc/ac stage is not studied here but further information can be found in [13]–[15].

III. VALIDATION OF THE TOPOLOGY USED

Some simulations have been carried out to check the correct operating of the topology introduced in Fig. 1.

The following hypotheses have been made in these simulations:

1) Two cascaded boost converters;
2) Three PV cells per converter;
3) Components are ideal;
4) The resistance *R*ch (see Fig. 2) simulates an inverter connected to the grid. The adaptation of its value allows us to extract the whole power;
5) PV cells have a voltage of 0.6 V and a current of 5 A under standard test conditions (STC);
6) The nominal duty cycle α of converters is 0.5;
7) Each boost operates in continuous conduction mode.

The simulation scheme is shown in Fig.

2. The different parameters and results are presented in Table I. The first simulation checks the nominal operating point (simulation1). All PV cells have the same operating point and the topology is able to extract the entire available power of each PV cell. Moreover, these simulations can be of interest to this topology in the case

of shadow. Indeed, simulation 2 illustrates a case where two PV generators have two different working points and shows that this topology is able to balance currents.

TABLE I
PARAMETERS AND RESULTS OF SIMULATION REALIZED WITH PSIM

	Simulation 1	Simulation 2	Simulation 3
Ve1	1.8 V	1.5 V	1.5 V
Ie1	5 A	2.5 A	1 A
Pe1	9 W	3.75 W	1.5 W
α1	0.5	0.646	0
Ve2	1.8 V	1.8 V	1.8 V
Ie2	5 A	5 A	5 A
Pe2	9 W	9 W	9 W
α2	0.5	0.292	0.75
Vs	7.2 V	7.2 V	7.2 V
Is	2.5 A	1.77 A	1.25 A
Ps	18 W	12.75 W	9 W

Every boost can supply the whole input power to the output, and is also able to regulate the output voltage at the desired value [12]. In this simulation, duty cycles are recalculated in order to obtain the same output voltage for unbalanced cases. For real cases, duty cycles will be tuned by using an individual MPPT. To study this system, it can be noted that the output current in a series string of converters must be equal, and the constraints for boost converters are Vin ≤ Vout and Iin ≥ Iout. A limit can appear when one PV generator is shaded; its current will fall. If this value is lower than the string output current, the string output current must be set to the value of the shaded cell current. In order to avoid this state, the topology is able to shunt the weak PV generator, thanks to the reverse diode of the MOSFET (simulation 3). In this case, all other cells can normally work and continue to provide the maximum of their energy. The weak cell(s) is (are) then shunted. Simulations have been carried out using PSIM software. They confirm that the topology can work in any rate of conditions, which is of real interest in the case of shadow.

IV. TOPOLOGY OPTIMIZATION

This study aims to adapt the PV modules and the converters for a grid-connected application. An optimization of the efficiency or the volume of the topology introduced in Fig. 1 has been accomplished. The goal of this optimization is to find the —*n*‖ and —*m*‖ pair to maximize produced energy. The number —*n*‖ is the number of cells to connect in series on the input of each boost and —*m*‖ is the number of boosts to cascade. This optimization must also define the optimum working point of the boost (frequency, input ripple current and input voltage). Fig. 3 shows the topology to optimize. The maximum number of cells is set in the first optimization to 144, which represents the number of cells of two current PV modules. This restriction limits the voltage ratio of the converters to 5 in order to decrease losses in the boost. A 5-in-multicrystalline cell has been used to realize this work (Photo watt, PW 1650, 165 W). The field of definition of the different parameters is defined in Table II. These values are directly set by the characteristics of the topology and its working constraints. Table II also defines the limits of the optimization and

the validity of models of losses and volumes that are developed in the next part.

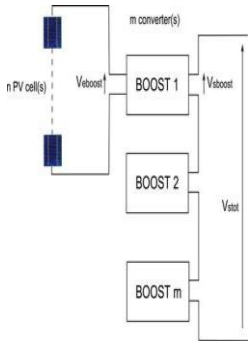

Fig. 3. Topology to optimize.

TABLE II
FIELD OF DEFINITION OF THE PARAMETERS

Parameter	Field of definition
n	1 < n < 144
m	1 < m < 144
n_{tot}	144
Frequency	20 kHz < F < 200 kHz
Input ripple current of boost	10 % < ΔI < 50 %
Input inductance of boost	0.9 µH < L < 6.5 mH
Semiconductor voltage rate	0 V < V < 400 V
Semiconductor current rate	5 A < I < 10 A
Cell current	5 A
Cell voltage	0.6 V
Duty cycle	0.76

The range of value of inductor ―*L*‖ is calculated in continuous-conduction mode.

Whatever the choice of the parameters ―*m*‖ or ―*n*,‖ the duty cycle α has the same value (0.76) corresponding to the cell input voltage (0.6 V) and the output voltage (360 V). Consequently, the value of *L* is determined with the ranges of parameters are defined in Table II.

V. MODELS OF LOSSES AND VOLUMES

A. Models of Losses

Losses in a boost converter are due to four components: the inductance, the MOSFET, the diode, and the capacitor. It is assumed that capacitor losses are neglected considering its weak influence in front of other components.

Concerning the semiconductor, conduction losses, switching losses and also Miller effect losses were modeled with the classical model.

TABLE III
MODELS OF THE VOLTAGE-DEPENDENT PARAMETERS

	Equations	
Losses in Mosfet	$R_{dson} = 1.51\times10^{-2}\times V_m - 0.1143$	(4)
	$C_{oss} = 5.33\times V_m^4 - 8.24\times10^{-18}\times V_m^3 + 4.11\times10^{-15}\times V_m^2 - 7.71\times10^{-13}\times V_m + 5.56\times10^{-11}$	(5)
Losses in Mosfet induced by diode	$I_{RM} = 5.6\times10^{-4}\times V_d^{1.59}$	(6)
	$C_d = 9.92\times10^{-10}\times V_d^{-.08}$	(7)
Losses in diode	$Q_{RR} = 1.30\times10^{-11}\times V_d^{1.42}$	(8)
	$V_F = 2.35\times10^{-3}\times V_d + 0.421$	(9)

An important work of modeling and normalization of the different parameters (*R*dson, *C*oss, *Cd* , *Q*RR, *I*RM, *VF*) has also been carried out to express losses in semiconductors [16]. This work is based on different datasheets of various manufacturers. Some hypotheses have been proposed. The current slope at the turn-on of the MOS is defined at the average value of 200 A·μs−1 and *t*off is fixed to 40 ns. *VF* is studied for a current of 5 A. In this case, previous parameters only depend on the voltage rating of the semiconductor and can be normalized according to this parameter. Therefore, the evolution of each influent parameter on the losses of semiconductors is known according to the voltage of the semiconductor. The equations of the model are shown in Table III. Concerning inductance losses, it has been necessary to recalculate them to obtain a table of values according to the frequency *F*, the ripple current

I, and also the inductance value *L*. To obtain the derivable function needed for the

optimization process, these results have been linearized using Featuring General Optimization Tool (FGOT) [20].

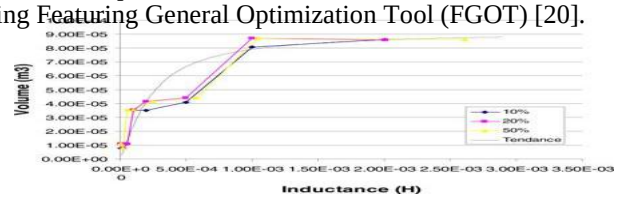

Fig. 4. Volume of inductor versus its value.

This equation is defined for the field of definition shown in Table II.

B. Models of Volume

The models of volume have been fitted by using some real cases sizing for heat sinks and inductors and by using datasheets for capacitors [16]. Basically, the volume of a semiconductor can be considered as the volume of the cooling system needed to refresh the chip. So, with datasheets of chips and heat sinks, an equation of the volume in function of needed thermal resistance has been defined

Vol rad = 5.68 × 10−4 × *R*thrad − 1.48. (1)

The switching frequency and current ripple have a negligible influence on this volume Vol *L* = 5912 × 10−5 × arctan(4.192 × 10−3 × *L*). (2)

Finally, the volume of the capacitor has been studied by referring to the datasheet values of electrolytic capacitors and it has been shown that the volume of the capacitor evolves linearly according to the applied voltage

Vol capa = 1.17 × 10−8 × *VC* + 3.13 × 10−7. (3)

VI. VALIDATION OF THE LOSSES MODELS

Before optimizing the topology, the model of losses presented in the previous section needs to be validated. So the results given by these models were compared to losses calculated

by the design of two real converters. The results are presented in Table IV.

TABLE IV

COMPARISON OF THE OPTIMIZATION AND THE DESIGN VALUES

	1 converter (F = 20 kHz, ΔI = 50 % and L = 1.313 mH)		8 converters (F = 37 kHz, ΔI = 17 % and L = 225 µH)	
	Calculated values	Optimization values	Calculated values	Optimization values
Losses in Mosfet	21 W	23,1 W	38,8 W	38,1W
Losses in diodes	1,8 W	2,1 W	4,8 W	5,15 W
Losses in inductance	3,44 W	2,5 W	3,3 W	4,02 W
Total losses	26.2 W	27,7 W	46,9 W	47,2 W

VII. OPTIMIZATIONS RESULTS WITHOUT SHADOW

Two optimizations were accomplished: the first one for the minimization of the volume of the converter and, the second one, for the maximization of European efficiency. This European efficiency takes into account the variation of the solar resource during one day and one year. This efficiency can be viewed like an energetic efficiency. Its expression is

$$\eta\text{euro} = 0.03 \times \eta 5 + 0.06 \times \eta 10 + 0.13 \times \eta 20 + 0.1 \times \eta 30 + 0.48 \times \eta 50 + 0.2 \times \eta 100 \quad (4)$$

where ηx is the efficiency at x% of the typical power [21]. The different optimizations have been carried out with the software CADES [22]. For this work, a determinist algorithm has been used. The results are shown in Table V.

A. Minimization of the Volume

The optimal solution when leading to a minimal volume is close to 10 converters. The frequency (122 kHz) and the input ripple current (50%) are much higher than the European efficiency optimization topology. The minimum volume is 235 cm3 . This volume is two times less than the volume of the optimized efficiency topology. The efficiency of this optimized volume topology falls to 87.1%. This volume optimization shows that volumes of the

optimized efficiency topology remain reasonable compare to the optimal volume. Moreover, the volume is less restrictive than efficiency. The available volume on the back of the PV module is enough to insert many converters. Consequently, only the efficiency will be taken into account in the following study.

VIII. FLEXIBLE DC/DC CONVERTER

According to the optimization results from Table VII, a dc/dc converter has been realized in order to validate the result of the optimized topologies. The converter has been built in two different ways. One way is to maximize the efficiency and the second way is to have a flexible converter which can run with a wide range of input/output voltage and power. The concept of a flexible converter is presented in [20].

A. Flexible Converter

The converter has to be able to accept a wide range of powers and input/output voltage values. All this work permits a converter which could be used for several sizes of PV modules, so with several powers and voltage values. The converter can boost input voltage value from below 7 V up to 450 V and can run from 6 to 500W.

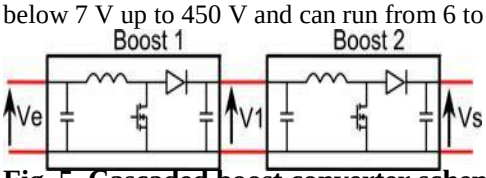

Fig. 5. Cascaded boost converter scheme.

TABLE V

CONFIGURATION OF THE CONVERTER VERSUS THE OPTIMIZATION RESULTS

Optimisation	Configuration of the converter
144 - linear	Cascaded Boost 1 and Boost2
144 - arcos	Boost 1
288 - linear	Boost 2
288 - arcos	Boost 1

In order to respond to this flexible function, the converter has been realized with two cascaded boosts as shown in Fig. 7 [10]. According to the input and output voltage values from the specifications, the converter makes possible the use of only a single boost or both. Each boost has been built on the same architecture; the differences between the two boosts are the current and voltage constraints on components. Connecting boosts in cascade with different ratings permits switching between several configurations according to the optimization shown in Table VIII.

B. Optimization of the Efficiency

The converter is built with the purpose of optimizing the efficiency without taking care of the volume. The only constraint imposed is the thickness which has to be lower than the aluminum frame of a PV module. In order to maximize the efficiency, technologies used for semiconductors are CoolMos and SiC diode. CoolMos gives better performances than traditional MOSFET in the switching and on-state losses [24]. The lower forward voltage drop and switching losses of the SiC Schottky diodes provide a better efficiency than the conventional silicon diode [25]. The first stage is realized with 100 V voltage rate components

(Vishay MOSFETSUP90N10-8m8P and Schottky diode16CTT100). The second one uses Infineon CoolMOS (IPP60R199CP) and SiC rectifier (SDT12S60). The two inductors have been realized with the same planar core (GER 44∗27∗10) and Litz wire (20 turns for the first boost and 30 turns for the second boost, and 0.8mm airgap for both). The frequency, the current ripple, and the inductance value are chosen according to the European efficiency optimization results (see Table V).

A microcontroller is used to control the converter which has the characteristic of being small and having very low consumption.

C. Experimental Tests

An MPPT program has been implanted in the device. The MPPT algorithm is based on the Hill Climbing method [26]. This method is simple, gives an accurate tracking of the maxi-mum power point, and can be easily programmed in a numerical control. Other new techniques of MPPT can improve the efficiency of the whole system [15]–[20].

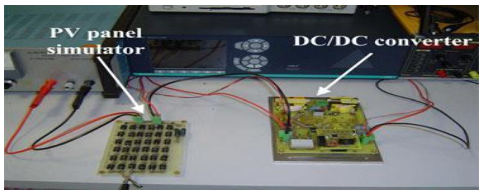

Fig. 6. DC/DC converter.

TABLE VI
TEST RESULTS

Optimisation	Maximal efficiency	European efficiency
144 - linear	96.80	95.78
144 - arctan	97.1	96.12
288 - linear	98.07	97.68
288 - arctan	98.10	97.26

Experimental test and measurement of the efficiency have been performed in order to compare to them simulation results. The results of this test are shown in Table IX. Experimental results are coherent with the optimization results. The converter (see Fig. 8) is able to work in all specifications given by the optimizations and maintain good efficiency.

IX. CONCLUSION

An optimization of a cascaded dc/dc converter devoted to grid-connected PV system

has been proposed. This converter is based on a boost chopper circuit. The correct operation and the advantages and the limits of this circuit have been checked by simulations on PSIM software. Models of losses and volume of the boost have been developed to realize the optimizations. However, the optimum depends on different parameters. To respond to these different variations, a flexible converter has been realized and tested. The experimental results confirm the extreme modularity and the good efficiency of this converter. A particular study for a PV generator of 144 cells has been done. Under these conditions, the best solution is a topology with two boosts and with 72 PV cells per boost. The study of the shadow effects on these topologies confirms these results. This optimum topology (with two boosts) is also the most efficient when the PV field is shaded. In a typical case (shadow of a chimney), it is able to produce 4% extra energy. The increase of the produced energy can reach up to 60% of the classical solution in the case of an important irradiation mismatch on the PV field. The properties of the PV field distributed topology are very interesting when the PV power generation systems have a partial shadowing issue. This distributed converter topology can strongly reduce the drawbacks related to building integrasted PV systems.

REFERENCES

[1] W.Hoffmann, ―PV on theway from a fewlead markets to aworld market,‖ in *Proc. IEEE 4th World Conf. Photovoltaic Energy Convers.*, May 2006, vol. 2, pp. 2454–2456.

[2] J. M. Carrasco, L. G. Franquelo, J. T. Bialasiewicz, E. Galvan, R. C. P. Guisado, Ma. A. M. Prats, J. I. Leon, and N. Moreno-Alfonso, ―Power electronics systems for the grid integration of renewable energy source—A survey,‖ *IEEE Trans. Ind. Electron.*, vol. 53, no. 4, pp. 1002–1016, Aug. 2006.

[3] M. Bachler, ―Grid connected systems in Europe— Looking into the future,‖in *Proc. IEEE 4th World Conf. Photovoltaic Energy Convers.*, May 2006, vol. 2, pp. 2289–2292.

[4] S. Liu and R. A. Dougal, ―Dynamic multiphysics models for solar array,‖*IEEE Trans. Ind. Electron*, vol. 17, no. 2, pp. 285–294, Jun. 2002.

[5] G. Petronea, G. Spagnuoloa, and M. Vitelli,

―Analytical model of mismatched photovoltaic fields by means of Lambert W-function,‖ *Solar Energy Mater. Solar Cells*, vol. 91, pp. 1652–1657, 2007.

[6] R. H. Bonn, ―Developing a ‗next generation‘ PV inverter,‖ in *Proc. IEEE Photovoltaic Spec. Conf.*, May 2002, pp. 1352–1355.

[7] G. Petrone, G. Spagnuolo, R. Teodorescu, M. Veerachary, and M. Vitelli, ―Reliability issues in photovoltaic power processing systems,‖ *IEEETrans. Ind. Electron*, vol. 55, no. 7, pp. 2569–2580, Jul. 2008.

[8] D. R. Neill and B.S.M. Granborg, ―Report on the photovoltaic R&D program in Hawaii,‖ *IEEE Trans. Energy Convers.*, vol. EC-1, no. 4, pp. 43–49, Dec. 1986.

[9] S. Rahman and M. Bouzguenda, ―A model to determine the degree of penetration and energy cost of large scale utility interactive photovoltaic systems,‖

IEEE Trans. Energy Convers, vol. 9, no. 2, pp. 224– 230, Jun.1994.

[10] G. R. Walker and P. C. Sernia, ―Cascaded DC– DC converter connection of photovoltaic modules,‖

IEEE Trans. Power Electron., vol. 19, no. 4, pp. 1130–1139, Jul. 2004.

[11] S. Cuk, ―Basics of switched mode power conversion: Topologies, magnetics and control,‖ in
Proc. IEEE Ind. Electron. Soc., 1991, pp. 265–269.

[12] A. Bratcu, I. Munteanu, S. Bacha, D. Picault, and B. Raison, ―Power optimization strategy for cascaded DC–DC converter topologies of photovoltaic modules,‖ presented at the IEEE International Conference on Industrial Technology, Gippsland, VIC, Australia, Feb. 2009.

[13] Y. Tsuchiya, ―A photovoltaic AC fusion converter,‖ *IEEE Trans. Energy Convers.*, vol. 14, no. 3, pp. 849–854, Sep. 1999.

[14] A. Ch.Kyritsis, E. C. Tatakis, and N. P. Papanikolaou, ―Optimum design of the current-source flyback inverter for decentralized grid-connected photovoltaic system,‖ *IEEE Trans. EnergyConvers.*, vol. 23, no. 1, pp. 281–293, Mar. 2008.

[15] B. Yang, W. Li, Y. Zhao, and X. He, ―Design and analysis of a gridconnected photovoltaic power system,‖ *IEEE Trans. Power Electron.*, vol. 25, no. 4, pp. 992–1000, Apr. 2010.

[16] S. Vighetti, ―Syst`emes photovolta¨ıques raccord´es au r´eseau: Choix et dimensionnement des ´etages de conversion,‖ Ph.D. dissertation, G2Elab, Grenoble Univ., Grenoble, France, 2010.

[17] G. Lef`evre, ―Conception de convertisseurs statiques pour l‘utilisation de la Pile `a Combustible,‖

Ph.D. dissertation, LEG, Grenoble Univ., Grenoble, France, 2004.

[18] G. Lef`evre,H.Chazal, J-P. Ferrieux, and

J.Roudet, ―Application ofDowell method for nanocrystalline toroid high frequency transformers,‖ presented at the IEEE Power Electronics Specialists Conference, Aachen, Germany, 2004.

[19] G. Lef`evre, J.-P. Ferrieux, J. Barbaroux, Ph. Boggetto, and P. Charlat, ―Minimizing magnetic components losses in a new DC–DC converter for portable fuel cell applications,‖ presented at the IEEE Industry Applications Society Conference, Seattle, WA, 2004.

[20] M. C. Costa and J.-L. Coulomb, ―An object-oriented optimization library for finite element method software,‖ *IEEE Trans. Magn.*, vol. 36, no. 4,pp. 1057–1060, Jul. 2000.

[21] J. M. A. Myrzik andM. Calais, ―String andmodule integrated inverters for single-phase grid connected photovoltaic systems—A review,‖ presented at the IEEE Power Tech Conference, Bologna, Italy, Jun. 2003.

[22] B. Delinchant, L. Estrabaut, L. Gerbaud, H. Nguyen Huu, B. Du Peloux, H.L. Rakotoarison,

F.Verdiere, and F.Wurtz, ―An optimizer using the software component paradigm for the optimization of engineering systems,‖ *Int. J. Comput. Math. Electr. Electron. Eng.*, vol. 26, no. 2, pp. 368–379, 2007.

[23] G. Yilei, H. Lijun, and L. Zhengyu, ―A flexible converter with two selectable topologies,‖ *IEEE Trans. Ind. Electron.*, vol. 56, no. 12, pp. 4465– 4472, Dec. 2009.